

# Surface plasma emission of small silver particles

M. P. Klyap, V. A. Kritskii, Yu. A. Kulyupin, M. A. Mukhtarov, K. N. Pilipchak, and S. S. Pop

*Physics Institute, Ukrainian Academy of Sciences*

(Submitted 21 November 1985)

*Zh. Eksp. Teor. Fiz.* **90**, 2137–2144 (June 1986)

The spectral, polarization, and angular characteristics of the radiation emitted by a silver-film island bombarded by slow electrons is investigated. The substantial role played by the substrate in the formation of the directivity pattern of the radiation produced by the radiative decay of surface plasmons in the small particles is demonstrated. It is shown that the angular dependence of the dipole-mode radiation intensity of surface plasma oscillations with vertically oriented dipole moment is nonmonotonic, in contrast to the case of radiation in a homogeneous medium.

## 1. INTRODUCTION

Interest in the electrodynamic properties of systems containing small metallic particles has greatly increased lately. The main reason is the observation of surface-enhanced Raman scattering of light<sup>1</sup> and surface second-harmonic generation.<sup>2</sup> In addition, research aimed at understanding the nature of the anomalous properties of "island" metallic films is being diligently pursued. The existence of the noted effects is attributed to excitation of natural surface oscillations of an electron gas in small metallic particles—surface plasma oscillations (SPO).

One of the basic still unanswered questions<sup>3,4</sup> is the role played by the substrate in the formation of the directivity pattern of the radiation due to radiative damping of the SPO in small metallic particles. We attack this question in this paper by using the electron-photon spectroscopy method,<sup>5,6</sup> which has been intensively developed in the last few years and has already yielded a number of important results. The

investigated objects were silver island films, to which most studies in this field are devoted.

## 2. MEASUREMENTS PROCEDURE AND RESULTS

The measurement of the spectral, polarization, and angular characteristics of plasma radiation of thin silver films was carried out with the electron-photon spectrometer described in detail in Ref. 7. The silver films were sputtered in the spectrometer chamber, at residual-gas pressure  $5 \cdot 10^{-6}$  Pa, on glass substrates coated with conducting carbon film 200 Å thick. The sputtering rate was about 1 Å/sec on a substrate heated to 350–400 °C, using an electron-beam heater placed on the back side of the substrate. The thickness of the sputtered silver layer was monitored with a quartz resonator. The film structure was investigated by a transmission electron microscopy; a film of weight thickness 50 Å is shown in Fig. 1. Histograms of the island distribution in size, constructed for a quantitative description of the structure, are shown in Fig. 2.

It can be concluded from electron-microscopy investigation of silver films, shaded by a chromium film, that islands up to 150–200 Å in size are close to spherical (for

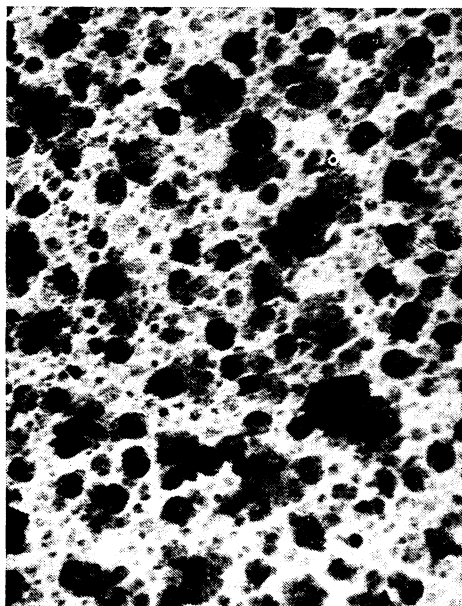


FIG. 1. Micrograms of the structure of a silver film with weight thickness 50 Å. Horizontal scale—300 Å/cm.

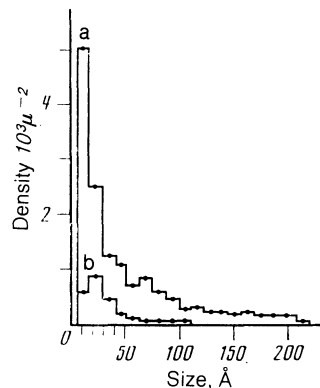


FIG. 2. Island distribution in size: a) for an island film with weight thickness 50 Å; b) for an island subsystem with distance  $L > 4a$  to the center of the nearest neighbor of the same size.

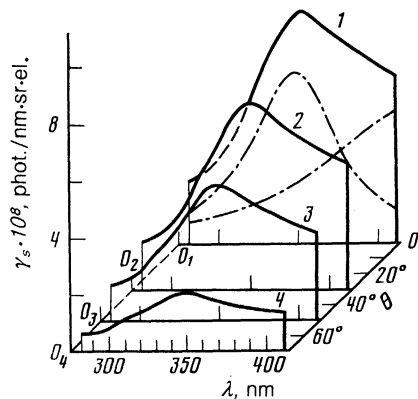


FIG. 3. Emission spectra of *s*-polarized light (solid lines) at various observation angles (electron incidence angle— $40^\circ$ , energy—500 eV). The dash-dot lines show the Lorentz components.

particles measuring about  $200 \text{ \AA}$  the oblateness of the sphere does not exceed 10%).

The working pressure in the experimental chamber was  $\sim 10^{-8}$  Pa. The design of the electron-photon spectrometer permitted independent measurement of the electron incidence angle  $\alpha$  and of the observation angle  $\theta$ . The energy  $E$  of the bombarding electrons was 100–500 eV. Further increase of the electron energy increased the substrate contribution to the recorded radiation, and the substrate contribution became predominant at  $E \geq 1000$  eV. The current density did not exceed  $1.7 \cdot 10^{-2}$  A/cm<sup>2</sup>, so that the bombardment did not lead to a noticeable heating of the investigated film.

Careful allowance for the photon-gathering geometry and for the spectral sensitivity of the spectrometer have permitted measurements of the absolute yield of the radiation. It was calculated by normalizing the measured number of photons to the value of the current passing through the target; this current depended on the electron incidence angles.

Figures 3 and 4 show by way of example the obtained light emission spectra for the *s*- and *p*-components at  $\alpha = 40^\circ$  and various observation angles. Similar plots were obtained at  $\alpha = 0$  and  $70^\circ$ . No corrections were introduced for the change of the light-source area with change of the observation angle, since the size of the glowing spot on the target was smaller than the optical image of the slit in the target plane.

### 3. DISCUSSION OF RESULTS

#### 3.1. Spectrum of natural oscillations

To estimate the quantum yield of the radiation as a result of radiative damping of various SPO, we must know their frequencies and damping. From the histogram of Fig. 2 (curve *a*) it follows that, in the system investigated, the radii of particles  $a$  lie in the range  $10^{-7}$ – $10^{-6}$  cm. The frequencies of solitary single silver particles of this size in vacuum, at not too high SPO mode numbers  $l$ , can be determined from the dispersion equation (see, e.g., Ref. 8)

$$\varepsilon = -(l+1)/l, \quad (1)$$

where  $\varepsilon$  is the dielectric constant of silver. In fact, the char-

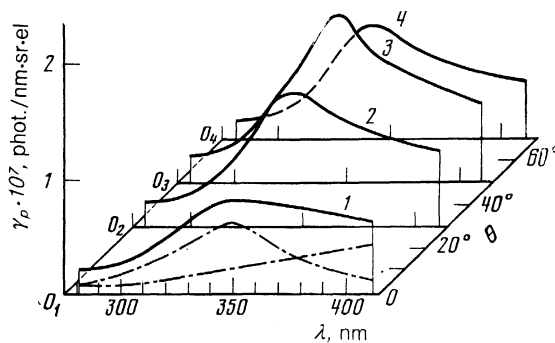


FIG. 4. Emission spectra of *p*-polarized light (solid lines) at various observation angles (electron incidence angle— $40^\circ$ , energy—500 eV). The dash-dot lines show the Lorentz components.

acteristic inhomogeneity of the  $l$ th SPO mode is of the order of  $l/a$ , so that in the range of parameters where the conditions

$$lv_F/(\omega_1 a) \ll 1, \quad \omega_1^2 a^2 / (lc)^2 \ll 1$$

are satisfied ( $v_F$  is the Fermi velocity and  $c$  is the speed of light) one can neglect in the SPO spectrum the nonlocality of the electromagnetic response of the electron gas and the time delay of the interaction. The SPO spectrum can consequently be determined in the local potential approximation to which Eq. (1) corresponds. In this approximation, using the data of Ref. 9 on the dielectric constant of silver, we obtain the energies  $\hbar\omega_1$  of the first three SPO modes for a solitary particle in vacuum, viz., 3.5, 3.58, and 3.61 eV.

In the system investigated, the silver particles are on a substrate whose presence can alter substantially the SPO frequencies compared with the case of a particle in a homogeneous medium.<sup>10</sup> The position of the maxima in the experimental emission spectra corresponds to an energy  $\hbar\omega \sim 3.5$  eV, which is close to the SPO frequency values cited above. It can be concluded therefore that under our experimental conditions the substrate does not affect significantly the SPO frequencies, a fact noted also earlier, e.g., in Ref. 4.

It must also be noted that for the film considered the average distance between particles of approximately the same dimension is comparable with this dimension. One can expect in this case a noticeable influence of a neighboring particle on the SPO spectrum. In Ref. 11 was calculated the spectrum of surface oscillations of a system consisting of two identical spheres, as a function of the distance between the particles. According to Ref. 11, with decreasing distance, the frequency of the coupled dipole oscillations decreases monotonically (in the case of a plasmalike dielectric constant of the sphere material) from the value corresponding to the frequency of the SPO dipole mode of a solitary sphere. Obviously, if the frequency shift due to the interaction with the neighboring particle does not exceed the half-width of the line corresponding to SPO dipole mode of a solitary particles, the coupled dipole oscillations emit in the same frequency interval as the solitary particle. According to Refs. 9 and 12, the damping of the SPO dipole mode of silver particles located in vacuum and having radii in the interval  $10^{-6}$ – $4 \cdot 10^{-7}$  cm is  $\text{Im}(\hbar\omega_1) \sim 0.1$  eV, so that the interaction does

not influence substantially the observed emission frequency if the distance between the particle centers exceeds triple the radius.<sup>11</sup> We used this attribute to separate a subsystem of "noninteracting" particles, for which the distance  $L$  to the center of the nearest particle of comparable size is not less than three, four, and six radii. Note that if the presence of a considerably smaller particle in the localization region of the SPO field of a given particle should not influence substantially the SPO frequency, since it alters the structure of the SPO field only in a region of the order of its own size. The particle distribution in size for the case  $L \gg 4a$  is shown by curve  $b$  of Fig. 2 (the distributions for other cases are similar in form).

### 3.2 Yield of radiation due to electron bombardment

The radiation intensity produced when a spherical metallic particle is bombarded by electrons was calculated in Refs. 3 and 4. In Ref. 13 were determined the probabilities of exciting various SPO modes and the quantum yield due to their radiative decay. No account was taken in the calculations of Refs. 13 and 14 of external-electron scattering not associated with SPO excitation. Obviously, this approximation is satisfactory for electrons that are fast enough and have a momentum mean free path exceeding the particle size. In the case of electrons of energy on the order of hundreds of electron volts, this path amounts in typical metals to several angstroms, so that scattering must be taken into account in the calculation of the SPO excitation. To our knowledge, however, this problem has not yet been solved.

Note that since the degree of localization of the SPO field is practically the same on both sides of the particle boundary, the probability of their excitation by electrons that pass through the particle (without a scattering that does not involve SPO excitation) and alongside the particle (within the confines of the SPO field) should be comparable. There is no short-range interaction for electrons passing alongside a particle and interacting with the SPO field. For these electrons, the conditions for a small change of the state upon excitation of the SPO, conditions assumed in the calculations of Refs. 13 and 14, should therefore be  $E \gg \hbar\omega_l$ ,  $P \gg \hbar l/a$  ( $P$  is the momentum of the exciting electron).

In view of the foregoing, we believe that it is possible to estimate the probability of SPO excitation by a flux of electrons of energy on the order of  $10^2$  eV, on the basis of calculations in which scattering is disregarded.

Comparison, on the basis of the calculation of Ref. 13, shows that the yield of photons due to radiative damping of the modes of a solitary particle in the vicinity of  $|\omega_l a/V| \lesssim 5$  ( $V$  is the exciting-electron velocity) of our experimental conditions ( $V \approx 1.3 \cdot 10^9$  cm/sec,  $a \lesssim 10^{-6}$  cm is smaller for the modes with  $l = 2$  and  $l = 3$  by about  $10^{-2}$  and  $10^{-5}$  times than the yield of the dipole mode  $l = 1$ ).

For this mode, the average number of photons emitted per incident electron is

$$N = W \frac{\gamma_R}{\gamma_T} = \frac{36\pi e^2 (\text{Re } \omega_l)^7 a^4}{\hbar (\text{Im } \omega_l + \gamma_R/2) \omega_p^2 V^2 c^3} f\left(\frac{\text{Re } \omega_l a}{V}\right), \quad (2)$$

where

$$W = \frac{108\pi e^2 a \omega_p}{\hbar V^2} \left(\frac{\text{Re } \omega_l}{\omega_p}\right)^3 f\left(\frac{\text{Re } \omega_l a}{V}\right)$$

is the average number of dipole-mode plasmons excited by one incident electron, and is obtained by integrating  $I_s(\omega)$  (Eq. (21) of Ref. 13) with respect to frequency under the condition  $|\text{Im } \omega_l / \text{Re } \omega_l| \ll 1$ ,  $\gamma_R = {}^2/3 (\text{Re } \omega_l)^4 a^3 c^{-3}$  is the probability of radiative decay per unit time,<sup>14</sup>  $\gamma_T = 2 \text{Im } \omega_l + \gamma_R$  is the total dipole-mode decay probability per unit time,

$$f(z) = \int_0^\infty j_1^2(x) x^{-3} dx,$$

$j_1(x)$  is a spherical Bessel function,  $e$  is the electron charge, and  $\omega_p$  is the plasma frequency.

To compare the calculated yield of the radiation at the dipole-mode frequency of a solitary particle with the measurements, account need be taken only of the particles that enter in "isolated" subsystems. The average number of photons due to radiative damping of the SPO dipole mode per electron is therefore of the order of

$$\bar{N} = \int N \sigma da,$$

where  $\sigma$  is the coverage of the film by particles having radii in the interval  $(a, a + da)$ ,  $N$  is given by Eq. (2), and the integration is over the subsystem of "noninteracting" particles. The quantities  $N$  calculated for distributions for which  $L \gg 3a$ ,  $L \gg 4a$ ,  $L \gg 6a$  have respective values of the order of  $5 \cdot 10^{-4}$ ,  $10^{-4}$ ,  $5 \cdot 10^{-6}$ .

The experimental quantum yield in the wavelength interval  $\Delta\lambda = 15$  nm, corresponding to the damping of the SPO dipole mode in solitary silver particles for which  $a \sim 4 \cdot 10^{-7}$  cm to  $10^{-6}$  cm near  $\lambda = 350$  nm, is of the order of  $10^{-5}$  photons per electron.

The order-of-magnitude agreement between the observed quantum yield and the calculated one (case  $L \gg 6a$ ) gives grounds for assuming that the observed radiation with maximum intensity at  $\lambda \approx 350$  nm is due to radiative decay of the SPO dipole mode.

### 3.3. Directivity pattern

The spectrum of the radiation due to radiative damping of various natural weakly damped electromagnetic oscillations of the system in the vicinity of the intensity-maximum can be fitted to a symmetric Lorentz curve. To separate the contribution made to the radiation by different natural modes we have therefore represented the experimental spectra as superpositions of symmetric Lorentz curves whose parameters were chosen to obtain best agreement with the experimental curve. Examples of the initial curve and of its "Lorentz spectrum" for the case when two Lorentz profiles are used for the approximation are shown in Figs. 3 and 4. Note that the parameters (maximum value, half-width, position of maximum) of the component whose center is close to  $\lambda \approx 350$  nm are practically independent of the number of components into which the initial curve is resolved.

Figure 5 shows the directivity pattern of a horizontal electric dipole located on a plane interface between vacuum

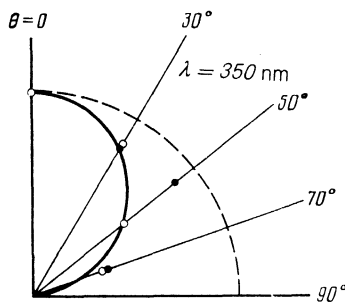


FIG. 5. Directivity pattern of horizontal electron plane on the plane vacuum-carbon interface in a plane perpendicular to the dipole moment. Solid curve—calculation, circles—experiment: ●— $\alpha = 0$ , ○— $\alpha = 40^\circ$ . The dashed line shows the directivity pattern in a homogeneous medium.

and a semi-infinite dielectric medium, when observed in a plane perpendicular to the dipole moment (the dashed line is the directivity pattern in a homogeneous medium). The dielectric constant of the medium is taken to be  $\epsilon_s = 3 + 3.6i$ , the value for amorphous carbon at a frequency  $\hbar\omega = 3.5$  eV (Ref. 15).<sup>1)</sup> The curve is based on the calculations of Ref. 3 (the coefficients of electromagnetic-wave reflection from opaque dielectrics were taken from Ref. 17). The circles in this figure represent the maximum values of the Lorentz component with center at  $\lambda \approx 350$  nm, obtained by resolving the  $s$ -polarization radiation spectra. It can be seen that the radiation intensity depends noticeably on the observation angle. We note also that the maximum radiation intensity, taken directly from the measured spectra without resolution into components, has a qualitatively similar angular dependence.

The fact that the radiation intensity depends on angle is evidence that the system containing the emitter has a preferred direction in the plane in which this dependence is measured. In our case this direction is the normal to the substrate surface (note that this is the only preferred direction in the system, since the substrate is isotropic in the interface plane, and the particles are randomly distributed).

The dependences of the intensity of  $s$ -polarized radiation on the observation angle is thus a consequence of the inhomogeneity of the medium in which the emitter is contained. The qualitative correspondence of the electric dipole on the interface (Fig. 5) to the directivity pattern confirms this conclusion.

The difference between calculation and experiment, which is particularly noticeable at oblique observation angles, is most likely due to reflection of the wave field from the carbon-glass interface or to the presence of other metallic particles in the near zone of the radiating dipole.

Figure 6 shows the directivity pattern of a vertical dipole located on the plane interface, for the same parameters as in Fig. 5 (the dashed curve is the directivity pattern in a homogeneous medium). The circles on this figure mark the values of the function

$$Y(\theta) = I_p(\theta) - I_p(0)F_p(\theta)/F_p(0),$$

where  $I_p(\theta)$  is the maximum value of the Lorentz component with center at  $\lambda \approx 350$  nm, obtained by resolving the  $p$ -

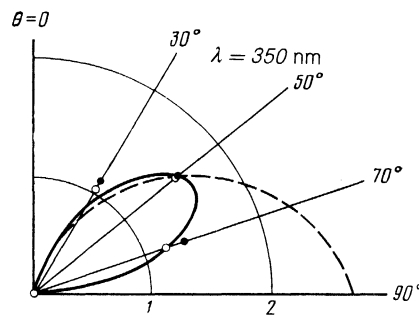


FIG. 6. Directivity pattern of vertical electric dipole on the plane vacuum-carbon interface in a plane containing the dipole moment. Solid curve—calculation, circles—values of  $Y(\theta)$ : ●— $\alpha = 0$ , ○— $\alpha = 40^\circ$ . The dashed line shows the directivity pattern in a homogeneous medium.

polarized radiation spectra, and  $F_p(\theta)$  is the radiation intensity, calculated in Ref. 3, of the horizontal dipole located on the boundary of the media and observed in the plane containing the normal to the interface and the dipole moment. The scale factor for  $Y(\theta)$  was chosen such that the point  $Y(50^\circ)$  was located on the curve.

Obviously, the function  $Y(\theta)$  describes the directivity pattern of the vertical dipoles in a system of incoherently emitting vertical and horizontal dipoles. This should be precisely the situation under our experimental conditions, inasmuch as during the time  $\Delta t \sim \gamma_R^{-1} \approx 3 \cdot 10^{-14}$  sec of emission of the SPO mode for this system of particles the electron that excites these oscillations is scattered and reverses direction repeatedly (mean path time  $\sim 10^{-16}$  sec). The orientation of the dipole moment of the excited oscillations is simultaneously reversed. It is therefore natural to expect the radiation observed at the frequency of the SPO dipole mode, which is the result of the averaging of the radiation of randomly oriented dipole moments, to be noncoherent. From this standpoint, it is also natural for the intensities of the dipole emission along the normal ( $\alpha = 40^\circ$ ) to be equal in polarizations parallel and perpendicular to the incidence plane, since the system is isotropic in the substrate plane, and the exciting electron "forgets" rapidly its initial direction.

It can be concluded from the results shown in Fig. 6 that that part of  $p$ -polarized radiation which corresponds to vertically oriented dipoles has an angular dependence (assuming that the horizontally oriented dipoles are described by the appropriate relation<sup>3)</sup> that corresponds qualitatively to the directivity pattern of a vertical dipole located on the plane interface of the media.

#### 4. CONCLUSION

Our analysis leads to the following conclusions: 1) Radiation with maximum intensity at  $\lambda \approx 350$  nm in both polarization is due to radiative decay of the SPO of a nearly spherical particle. 2) The substrate influences substantially the angular dependence of the dipole-radiation intensity.

The second conclusion agrees with the results of Ref. 3 and contradicts the statement<sup>4)</sup> that the substrate does not influence significantly the directivity pattern of the radiation due to radiative damping of the SPO. We note, however, that Ref. 4 does not contain enough information on the radiation

intensity at  $\theta \gtrsim 60^\circ$ , where the role of the substrate should become most pronounced.

<sup>1)</sup>A noticeably different value  $\epsilon_s \approx 1.6 + 4.2i$  was obtained in Ref. 16 for the dielectric constant of amorphous carbon at the same frequency. However, the difference (larger for oblique observation angles) between the directivity patterns of Figs. 5 and 6 for these two values of  $\epsilon_s$  does not exceed 10% in amplitude at angles up to  $80^\circ$ .

<sup>1</sup>Surface Enhanced Raman Scattering, R. K. Chang and T. E. Furtak, eds., Plenum, 1982.

<sup>2</sup>A. Wokaun, J. G. Bergman, J. P. Heritage, A. M. Glass, P. F. Liao, and D. H. Olson, Phys. Rev. B **24**, 849 (1981).

<sup>3</sup>W. Lukosz, J. Opt. Soc. Am. **69**, 1495 (1979).

<sup>4</sup>J. W. Little, T. A. Callcott, T. L. Ferrell, and E. T. Arakawa, Phys. Rev. B **29**, 1606 (1984).

<sup>5</sup>M. P. Klyapp, V. A. Kritskii, Yu. A. Kulyupin, Yu. N. Kucherenko, K. N. Pilipchak, and S. S. Pop, Zh. Eksp. Teor. Fiz. **86**, 1117 (1984) [Sov.

Phys. JETP **59**, 653 (1984)].

<sup>6</sup>D. P. Woodruff, N. V. Smith, P. D. Johnson, and W. A. Royer, Phys. Rev. B **26**, 2943 (1982).

<sup>7</sup>V. A. Kritskii, M. P. Klyapp, and S. S. Pop, Prib. Tekh. Eksp. No. 3, 149 (1985).

<sup>8</sup>R. Ruppin and R. Englman, J. Phys. C **1**, 630 (1968).

<sup>9</sup>P. B. Johnson and R. W. Christy, Phys. Rev. B **6**, 4370 (1972).

<sup>10</sup>R. Ruppin, Surf. Sci. **127**, 108 (1983).

<sup>11</sup>R. Ruppin, Phys. Rev. B **26**, 3440 (1982).

<sup>12</sup>A. Kawabata and R. Kubo, J. Phys. Soc. Jpn. **21**, 1765 (1966).

<sup>13</sup>I. Fujimoto and K. Komaki, *ibid.* **25**, 1679 (1968).

<sup>14</sup>J. Crowell and R. H. Ritchie, Phys. Rev. **172**, 436 (1968).

<sup>15</sup>E. T. Arakawa, M. W. Williams, and T. Inagaki, J. Appl. Phys. **48**, 3176 (1977).

<sup>16</sup>G. Jungk and C. H. Lange, Phys. Stat. Sol. B **50**, K71 (1972).

<sup>17</sup>J. A. Stratton, *Electromagnetic Theory*, McGraw, 1942, Chap. 11 (Russ. transl. IL, 1948, pp. 445-446).

Translated by J. G. Adashko